Frequency Stabilization of a Cesium Faraday Laser With a Double-Layer Vapor Cell as Frequency Reference

Hangbo Shi, Pengyuan Chang, Zhiyang Wang, Zijie Liu, Tiantian Shi, *Member, IEEE*, and Jingbiao Chen

***Abstract*—We implement a compact optical frequency standard at the wavelength of 852 nm by the modulation transfer spectroscopy (MTS) technique, using a Faraday laser as the local oscillator and a double-layer cesium vapor cell to provide frequency reference. The vacuum space between the two quartz glass layers of the double-layer atomic vapor cell can effectively suppress the temperature fluctuations inside the internal atomic vapor cell. The influences of probe and pump laser powers, modulation frequency, and vapor cell temperature on the slope of the MTS error signal are measured. Utilizing the self-estimation method, we evaluate the frequency stability of the laser system, which can be up to $5.8 \times 10^{-15}/\sqrt{\tau}$ at short term, dropping to 2.0×10^{-15} at 50 s. This result is obviously superior to that using single-layer vapor cell as the frequency reference. Such an ultrastable laser source can be widely used in the fields of optical metrology and precision measurement.**

***Index Terms*—Frequency standard, Faraday laser, modulation transfer spectroscopy, double-layer vapor cell.**

I. Introduction

FREQUENCY-STABILIZED external-cavity diode lasers (ECDLs) with narrow linewidth and high-frequency stability are key pieces of technology in a number of diverse applications, such as atomic clocks [1], atomic gravimeters [2], and atomic magnetometers [3], [4]. ECDLs use frequency selective feedback to achieve narrow linewidth and good tunability. Various frequency selection elements, such as gratings [5], [6], interference filters [7], [8], Fabry-Perot etalons [9], [10], are used for narrow-bandwidth filtering. Although the above ECDLs can realize single-mode laser with narrow linewidth and good tunability, their frequencies are susceptible to mechanical vibrations and changes in the current and temperature of laser diodes. Furthermore, after long-time operation, the frequency shift of the ECDLs above is inevitable. Therefore, the laser frequency should be calibrated, which is inconvenient.

Faraday anomalous dispersion optical filter (FADOF), first proposed in 1956 [11], plays an important role in frequency selecting and optical communication systems owing to its narrow bandwidth, high transmission and high noise rejection ratio. Only the laser frequency within a narrow frequency range near the atomic transition can be transmitted.

The ECDL utilizing FADOF as frequency-selecting element [12], [13] is immune to mechanical vibrations and exhibits good long-term frequency stability. The reason is that it uses the atomic transition as an absolute reference for frequency selection, that is, only the laser mode within the transmission spectrum of the FADOF can survive, and the laser frequency is limited to a narrow range. However, the frequency of such an ECDL hops markedly when the current and temperature of the laser diode change over a wide range, owing to internal-cavity modes. The "Faraday laser" with an antireflection coated laser diode (ARLD) as gain medium, which is for eliminating the internal cavity modes, was first achieved in 2011 [14]. Thus, the frequency of the Faraday laser is insusceptible to the changes in the current and temperature of the laser diode, and the Faraday laser has been widely studied due to its excellent properties [14], [15], [16], [17], [18].

To further optimize the laser frequency, the ECDLs are stabilized by saturation absorption spectroscopy (SAS) [19], polarization spectroscopy (PS) [20], [21], modulation transfer spectroscopy (MTS) [22], [23], [24], [25], [26], [27], [28], [29], dichroic atomic vapor laser lock (DAVLL) [30], [31], [32], Pound-Drever-Hall (PDH) technique [33], [34], etc. In this work, we use MTS for frequency stabilization. On the one hand, compared with SAS, PS, and DAVLL, MTS has several advantages as following. The spectral signal of MTS is background-free due to the nonlinear interaction between photons and atoms; therefore, the zero point of the dispersive-like signal is insusceptible to ambient temperature, intensity of laser, etc. Furthermore, the laser frequency is modulated with high modulation frequency by electro-optic modulator (EOM), so low-frequency noise can be effectively suppressed. On the other hand, compared with PDH, the MTS system has the advantages of significantly

Manuscript received 26 October 2022; accepted 6 November 2022. Date of publication 15 November 2022; date of current version 29 November 2022. This work was supported in part by the National Natural Science Foundation of China (NSFC) under Grant 91436210, in part by the China Postdoctoral Science Foundation under Grant BX2021020, and in part by the Wenzhou Major Science & Technology Innovation Key Project under Grant ZG2020046. *(Corresponding author: Tiantian Shi.)*

Hangbo Shi, Zhiyang Wang, Zijie Liu, Tiantian Shi, and Jingbiao Chen are with the State Key Laboratory of Advanced Optical Communication Systems and Networks, School of Electronics, Peking University, Beijing 100871, China (e-mail: shihangbo@stu.pku.edu.cn; wzy_sxn@stu.pku.edu.cn; lzj871622534@126.com; tts@pku.edu.cn; jbchen@pku.edu.cn).

Pengyuan Chang is with the State Key Laboratory of Advanced Optical Communication Systems and Networks, School of Electronics, Peking University, Beijing 100871, China, and also with Institute of Quantum Information and Technology, Nanjing University of Posts and Telecommunications, Nanjing 210003, China (e-mail: cpyxm@pku.edu.cn).

Digital Object Identifier 10.1109/JPHOT.2022.3221494

reduced volume and cost, extending its application scope. Moreover, MTS can also achieve better long-term stability since the laser frequency is locked to the quantum transition frequency rather than a supercavity with PDH technique. Thus, the MTS technique is widely used. For example, the 532 nm I_2 optical frequency standard based on MTS technique has been selected as a wavelength standard with high frequency stability [24], [25]. Klaus Döringshoff et al. operated the I_2 frequency standard in space on a sounding rocket mission with frequency stability of $1.5 \times 10^{-13}/\sqrt{\tau}$ [28]. Shang et al. realized an 852 nm frequency standard whose frequency stability measured via beat detection is 4.8×10^{-13} at 1 s [35]. Chang et al. implemented an 852 nm frequency standard with self-estimated frequency stability of $3 \times 10^{-14}/\sqrt{\tau}$ based on the Faraday laser [36].

However, the temperature of the atomic vapor cell in MTS fluctuates chronically, limiting long-term frequency stability. Current frequency stabilization methods commonly use single-layer atomic vapor cells as frequency reference, which cannot inhibit temperature fluctuations well. The double-layer atomic vapor cell provides a vacuum space between two layers of quartz glass, which can effectively reduce the thermal conduction between the vapor cell and the ambient air, successfully solving the problem of temperature fluctuations of the atomic vapor cell. Therefore, we utilize the double-layer atomic vapor cell as the frequency reference, and the experimental result shows that the stability of the laser frequency is clearly improved compared with that of the single-layer atomic vapor cell.

Here, we stabilize the frequency of the Faraday laser by MTS, utilizing a double-layer atomic vapor cell as the frequency reference, then we implement an 852 nm compact optical frequency standard system. In this system, the frequency of the laser is stabilized on the cycling transition ($6\,s^2S_{1/2}|F = 4\rangle - 6p^2P_{3/2}|F' = 5\rangle$) at cesium 852 nm wavelength. We use the self-estimation method [37], [38], [39], [40] to evaluate the frequency stability, which is $5.8 \times 10^{-15}/\sqrt{\tau}$ at short term, dropping to 2.0×10^{-15} with an averaging time of 50 s.

II. Experimental Setup and Methods

The experimental setup is shown in Fig. 1(a). The Faraday laser is used as the local oscillator. A FADOF which consists of two polarization beam splitters (PBSs), a cesium vapor cell (cell1), and NdFeB magnets, is used for frequency selection. The cell1, with a length of 3 cm and a diameter of 1.5 cm, is filled with cesium and 10 torr Ar buffer gas, heated by a twisted copper heating wire and enclosed by Teflon layers for thermal insulation. The 10 torr Ar buffer gas can broaden the full width at half maximum (FWHM) of the transmission spectrum of FADOF, which broadens the mode-hop-free tuning range of the Faraday laser. The temperature of cell1 is controlled at 72 °C within 0.1 °C to fix the cesium saturated vapor pressure inside the cell1. The NdFeB magnets are placed around the cell1 to provide an axial magnetic field with a center of 900 G. The light is emitted from an anti-reflection coated laser diode (ARLD, Toptica EYP-RWE-0860-06010-1500-SOT02-0000), which can eliminate the internal-cavity modes. The first PBS is used to generate line polarized light, and the light's polarization rotates after the

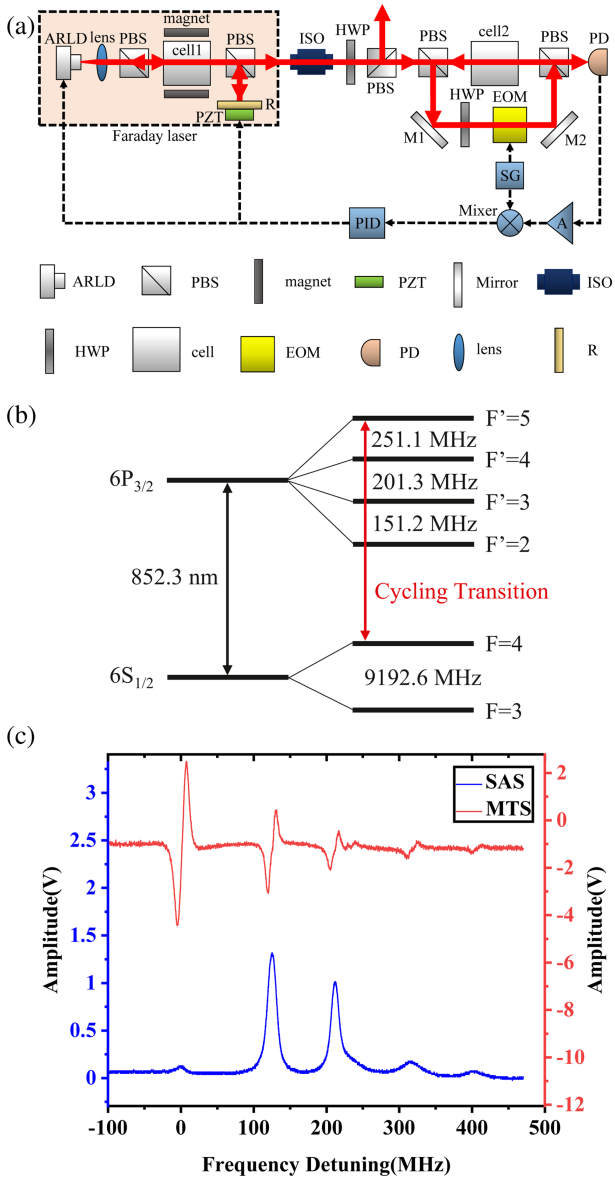

Fig. 1. (a) Experimental setup. ARLD: anti-reflection coated laser diode, PBS: polarization beam splitter, cell1: cesium vapor cell of the Faraday laser, R: high-reflection mirror, PZT: piezoelectric transducer, ISO: isolator, HWP: half wave plate, cell2: double-layer cesium vapor cell of the MTS system, EOM: electro-optic modulator, PD: photoelectric detector, SG: signal generator, A: amplifier, PID: proportional integral derivative controller. (b) Cesium energy level diagram. (c) SAS (solid blue line) and corresponding MTS (solid red line) of the transition of $6\,s^2S_{1/2}|F = 4\rangle - 6p^2P_{3/2}$.

light passes through the cesium vapor cell due to the Faraday effect. Only the light whose polarization rotates 90° can pass the second PBS, which is selected from a narrow frequency range corresponding to the atomic resonance line. The light is reflected at the high-reflection mirror (R) for optical feedback. Subsequently, the light passes through the FADOF for frequency selection agian, then back into the ARLD for optical amplification, reflected by the reflective surface of the ARLD and once again passing through the FADOF. After continuous optical feedback, frequency selection and optical amplification, the laser coherence is improved with linewidth narrowing. The cavity

Fig. 2. Double-layer vapor cell (left) and the single-layer vapor cell (right). The double-layer atomic vapor cell has a vacuum space between two layers of quartz glass, effectively reducing the thermal conduction between the vapor cell and the ambient air. The length and the diameter of the double-layer vapor cell are 11 cm and 2.6 cm, respectively. The length and the diameter of the single-layer vapor cell are 10 cm and 2 cm, respectively.

length of the Faraday laser is $L = 15.5$ cm, and the free spectrum range (FSR) is given by $FSR = c/2\,L = 967.74$ MHz, where c is the light speed. The piezoelectric transducer (PZT) is attached to the output coupling mirror to adjust the cavity length so that the laser frequency could be tuned. In this experiment, we tune the laser frequency near the transition of $6\,s^2S_{1/2}|F = 4\rangle - 6p^2P_{3/2}$ (see Fig. 1(b)). The laser emitted from the Faraday laser is split into two beams by the PBS, used as probe laser and pump laser, respectively. A half wave plate (HWP) is placed in front of the PBS to control the ratio of the pump and the probe laser power. The pump laser is phase modulated by an EOM. A HWP is placed in front of the EOM to make the polarization direction of the pump laser parallel to the principal axis of the EOM. The temperature of the EOM in this system is controlled at 25 °C by a thermoelectric cooler (TEC) that allows to maintain the temperature of the EOM within 0.1 °C, in order to reduce the residual amplitude modulation (RAM). The probe laser is detected by a photoelectric detector (PD, Thorlabs PDA8A/M). The saturation absorption spectrum is shown in Fig. 1(c). In order to minimize the temperature fluctuations inside the cesium vapor cell of MTS, a double-layer vapor cell (see Fig. 2) with a vacuum space between the two quartz layers (cell2) is used as the frequency reference. The cell2 is filled with pure cesium. The temperature of the cell2 is controlled with a heating wire around it. And the cell2 is placed in a box consisting of Teflon layers and permalloy layers for thermal insulation and magnetic shielding, respectively. The signal detected by the PD is amplified by an amplifier (A, Mini-Circuits ZFL-500LN+), subsequently demodulated by a mixer (Mini-Circuits ZFM-2-S+) with a radio-frequency (RF) signal, and finally we can get the modulation transfer spectrum, as shown in Fig. 1(c). The demodulated signal, utilized as residual error signal, is fed back to the Faraday laser by a proportional integral derivative

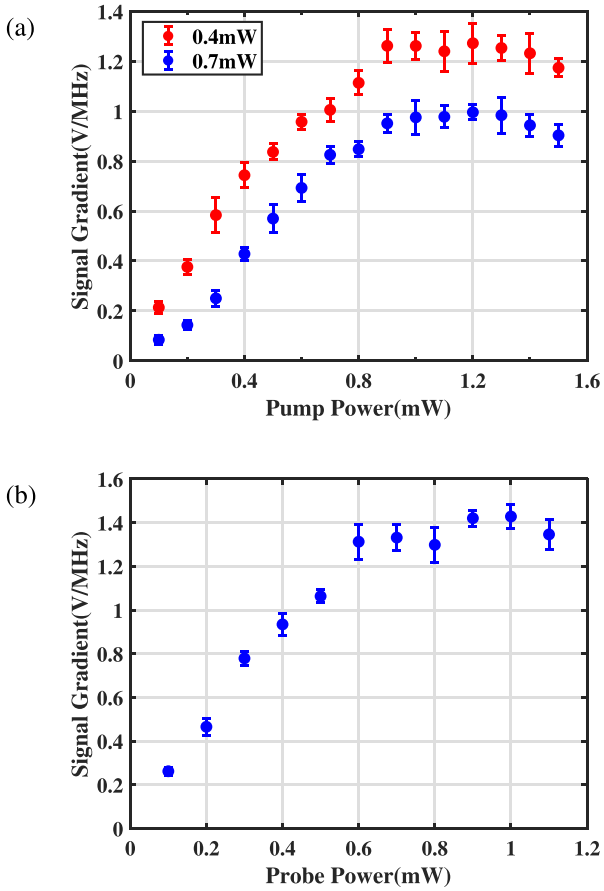

Fig. 3. (a) Influence of the pump laser power on the slope of the MTS signal when the probe laser power is 0.4 mW (red) and 0.7 mW (blue) respectively. (b) Influence of the probe laser power on the slope of the MTS signal when the pump laser power is fixed at 0.9 mW.

(PID) controller (Vescent D2-125) for frequency stabilization. The frequency of the Faraday laser can be continuously tuned within the Doppler spectrum. However, we just use the hyperfine transition of $6\,s^2S_{1/2}|F = 4\rangle - 6p^2P_{3/2}|F' = 5\rangle$ to lock the frequency of the Faraday laser, because it is corresponding to the largest gradient of MTS signal in all the SAS peaks of the transition of $6\,s^2S_{1/2}|F = 4\rangle - 6p^2P_{3/2}$, leading to a better frequency stability. The whole laser system occupies a space of $44 \times 40 \times 10.5$ cm^3.

III. Results and Analysis

We investigate the dependence of the slope of the MTS signal corresponding to the hyperfine transition of $6\,s^2S_{1/2}|F = 4\rangle - 6p^2P_{3/2}|F' = 5\rangle$ on the probe and pump laser powers, to optimize the resolution and sensitivity of the servo-loop. Fig. 3(a) shows the influence of the pump laser power on the slope of the MTS signal when the probe laser power is 0.4 mW and 0.7 mW, respectively. When the pump laser power is low, the peak-to-peak amplitude of the MTS signal has an upward trend with the pump light power going up so that the slope of the MTS signal gradually increases. The MTS signal saturates when the pump laser power goes up to a certain extent so

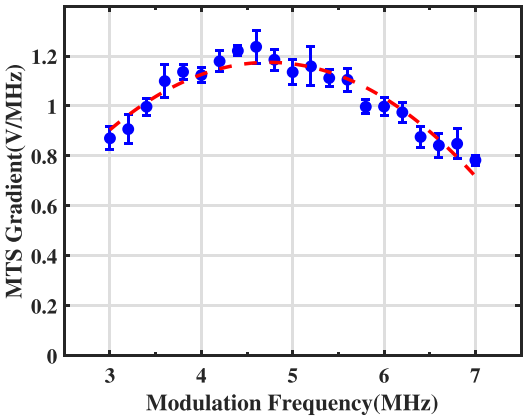

Fig. 4. Influence of modulation frequency on the slope of the MTS signal when the probe and pump laser powers is fixed at 0.7 mW and 0.9 mW respectively. The dash line is the polynomial fitting of the experimental data.

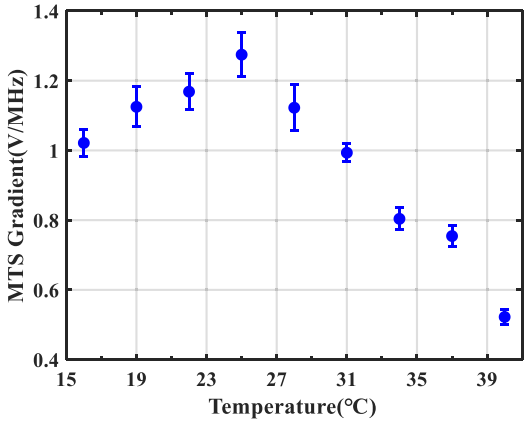

Fig. 5. Influence of temperature in the double-layer vapor cell on the slope of the MTS signal.

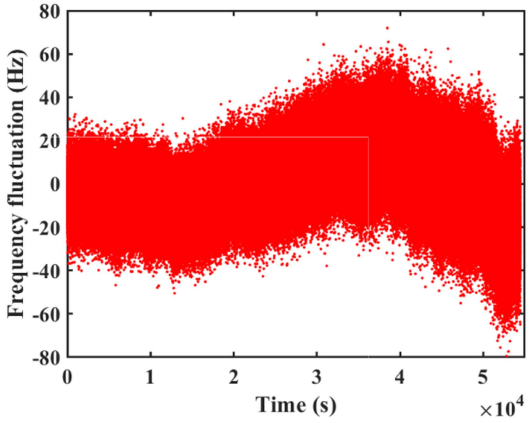

Fig. 6. Time series of the frequency fluctuations described by residual error signal.

that the peak-to-peak amplitude of the MTS signal no longer increases, while the power broadening becomes more and more significant, making the peak-to-peak frequency interval of the MTS signal larger and larger. That is to say, the slope of the MTS signal gradually decreases. Thus, in our system, we fix the pump laser power at 0.9 mW and then investigate the influence of probe laser power on the slope of the MTS signal, as shown in Fig. 3(b). When the probe laser power is low, the peak-to-peak frequency interval of the MTS signal is almost irrelevant to the probe laser power. However, as the pump laser power going up, the peak-to-peak amplitude of the MTS signal increases, giving rise to the increase in the slope of the MTS signal. As the probe laser power continues to get higher and higher, the slope of the MTS signal becomes steady due to the gradual saturation of the peak-to-peak amplitude and the increasing power broadening. Consequently, the probe laser power in our setup is set at 0.7 mW. We exclude the higher power because, based on repeated experiments, higher stability is not achieved when the power is beyond 0.7 mW, probably due to the excess noise brought in by the high-power probe laser.

With the probe and pump laser powers fixed at 0.7 mW and 0.9 mW respectively, we measure the variation regularity of the slope of the MTS signal as the modulation frequency goes up, as shown in Fig. 4. With the increase in the modulation frequency, the slope of the MTS signal increases to a peak value at 4.6 MHz and goes down afterwards, for the reason that the peak to peak amplitude first increases to a maximum value and then decreases. Thus, for the optimal locking performance, the modulation frequency is set at 4.6 MHz in our system.

A suitable temperature is also needed for the vapor cell to achieve optimal stability. As shown in Fig. 5, the slope of the MTS signal increases and subsequently decreases as the temperature of the cesium vapor cell increases. Under the condition of low temperature, the slope of the MTS signal has an upward trend with the rise of the temperature, because the increase in the saturation vapor pressure makes the cesium atomic density in the vapor cell go up. The slope of the MTS signal drops sharply when the vapor cell temperature continues to increase, because the collisional broadening becomes more and more significant, making the spectral line width of SAS signal and the peak-to-peak frequency interval of MTS signal larger and larger, far beyond the increase in the peak-to-peak amplitude. The slope of the MTS signal peaks at $25\,^{\circ}\mathrm{C}$ so that the temperature of the vapor cell is fixed at $25\,^{\circ}\mathrm{C}$.

After all the experimental conditions are optimized, the Faraday laser is locked on the cycling transition $(6\,s^2S_{1/2}|F=4\rangle - 6p^2P_{3/2}|F'=5\rangle)$ with MTS technique, by feeding the residual error signal back to the controller of the Faraday laser (PZT and current ports) for slow-speed servo and directly back to the laser diode port for high-speed servo. Fig. 6 shows the time series of frequency fluctuations, which is described by the residual error signal. The frequency stability of the Faraday laser is evaluated by the self-estimation method, as shown in Fig. 7. When we use double-layer vapor cell as the frequency reference, the short-term frequency stability of the Faraday laser is $5.8 \times 10^{-15}/\sqrt{\tau}$, decreasing to 2.0×10^{-15} at 50 s. After replacing the single-layer vapor cell with a double-layer vapor cell, the short-term stability of the laser system is optimized from $8.3 \times 10^{-15}/\sqrt{\tau}$ to $5.8 \times 10^{-15}/\sqrt{\tau}$. The long-term stability of the laser system using a double-layer vapor cell is 2 to 3 times

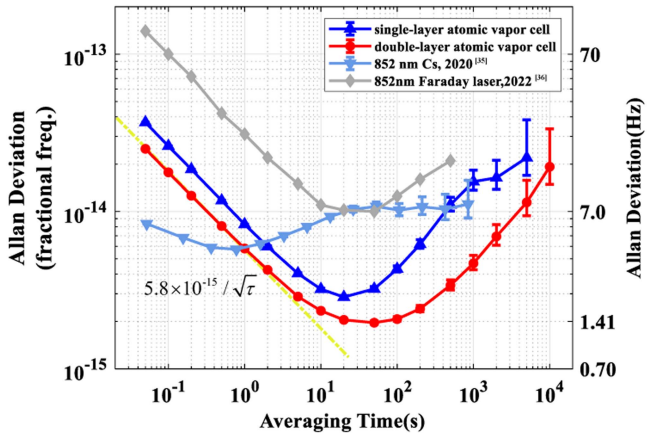

Fig. 7. Comparison of Allan deviations of several laser systems. The left and the right ordinates indicate the fractional frequency stability and the absolute frequency stability, respectively. The dark blue and the red lines represent the Allan deviations of the system when a single-layer and a double-layer vapor cells are used in our setup, respectively. The light blue line shows the Allan deviation of the compact 852 nm cesium optical standard in [35]. The gray line represents the 852 nm Faraday laser in [36].

that of the laser system using a single-layer vapor cell, and the averaging time when the Allan deviation starts to deteriorate of the former is 2.5 times as long as that of the latter. We can see that both the short-term and long-term stabilities of the system using a double-layer vapor cell are much higher than those of the system using a single-layer vapor cell, especially in terms of long-term stability, which shows the significant effect of the double-layer vapor cell. This reason is that the long-term stability of the system is mainly limited to the temperature fluctuations inside the vapor cell. The temperature fluctuations inside the vapor cell cause the ups and downs in saturation vapor pressure, then the atomic density within the vapor cell changes, leading to the variation of the transmittance. Therefore, the error signal fluctuates when the laser frequency does not drift at all. Furthermore, the collisional broadening effect and the collisional shift effect can be expressed respectively as

$$\Delta\omega = 2n_0\sigma'\bar{v},$$
$$\delta\omega = n_0\sigma''\bar{v}, \tag{1}$$

where n_0 is the atomic density, σ' is the collisional broadening cross-section, σ'' is the collisional shift cross-section, and $\bar{v}$ is the mean relative velocity. As the temperature fluctuates, n_0 and $\bar{v}$ within the vapor cell change, and therefore $\Delta\omega$ and $\delta\omega$ cannot stay the same, resulting in the drift of the reference frequency and the variation of the slope of the MTS signal. That is to say, the stability will deteriorate, especially the long-term one, as a result of low-frequency temperature fluctuations inside the vapor cell. It is noteworthy that the double-layer vapor cell provides a vacuum space between two quartz layers, which can commendably isolate the interior of the atomic vapor cell from the external environment, thus greatly weakening the temperature variation. In other words, the temperature of the cesium atoms inside the vapor cell cannot keep up with the outside temperature change, thus significantly reducing the temperature fluctuations inside the vapor cell. As a consequence, the long-term stability of the system is greatly improved by using a double-layer vapor cell. Meanwhile, the long-term stability of our system performs much better than the compact 852 nm Cs optical standard in [35]. The averaging time when the Allan deviation curve is starts to deteriorate of our system is 50 times as long as that of the system in [35]. Compared with the 852 nm Faraday laser in [36], the frequency stability of our system is about 4 times better both in the long-term and the short-term scales. In addition, because of the improved long-term stability, the laser frequency can be locked for at least three days, and the system can be used in outdoor applications with large temperature fluctuations.

IV. Conclusion

We realize an 852 nm compact optical frequency standard system on the basis of the MTS technique. A Faraday laser is utilized as the local oscillator, and in order to inhibit the temperature drift inside the vapor cell, we utilize a double-layer cesium vapor cell as the frequency reference. We study the factors of the slope of the MTS signal, such as probe and pump laser powers, modulation frequency, and vapor cell temperature, and then set these factors at the optimal values. By the self-estimation method, the preliminary stability of the frequency standard is $5.8 \times 10^{-15}/\sqrt{\tau}$, decreasing to 2.0×10^{-15} at 50 s, which performs much better than the laser system with a single-layer vapor cell. We find great potential of this frequency-stabilized laser system, which is a promising alternative to PDH technology in the future, with significantly reduced cost and size. And it can be widely used in many fields, such as atomic clocks, atomic gravimeters, atomic magnetometers, etc. In our future work, we will further improve the temperature-control equipment of the vapor cell and fix the double-layer vapor cell in an adiabatic vacuum chamber so that the long-term stability of the system might continue to be optimized. The stability of the system will be evaluated by optical heterodyne beating between two identical frequency-stabilized laser systems.

References

[1] K. Bongs et al., "Development of a strontium optical lattice clock for the SOC mission on the ISS," *C. R. Phys.*, vol. 16, no. 5, pp. 553–564, 2015.
[2] Z. Hu et al., "Demonstration of an ultrahigh-sensitivity atom-interferometry absolute gravimeter," *Phys. Rev. A*, vol. 88, no. 4, 2013, Art. no. 043610.
[3] N. Behbood, F. M. Ciurana, G. Colangelo, M. Napolitano, M. W. Mitchell, and R. J. Sewell, "Real-time vector field tracking with a cold-atom magnetometer," *Appl. Phys. Lett.*, vol. 102, no. 17, 2013, Art. no. 173504.
[4] D. Budker and M. Romalis, "Optical magnetometry," *Nature Phys.*, vol. 3, pp. 227–234, 2007.
[5] K. Liu and M. G. Littman, "Novel geometry for single-mode scanning of tunable lasers," *Opt. Lett.*, vol. 6, no. 3, pp. 117–118, 1981.
[6] L. Ricci et al., "A compact grating-stabilized diode laser system for atomic physics," *Opt. Commun.*, vol. 117, no. 5, pp. 541–549, 1995.
[7] M. Gilowski et al., "Narrow bandwidth interference filter-stabilized diode laser systems for the manipulation of neutral atoms," *Opt. Commun.*, vol. 280, no. 2, pp. 443–447, 2007.
[8] L. Zhang et al., "Development of an interference filter-stabilized external-cavity diode laser for space applications," *Photonics*, vol. 7, no. 1, 2020, Art. no. 12.
[9] B. E. Bernacki, P. R. Hemmer, S. P. Smith, and S. Ezekiel, "Alignment-insensitive technique for wideband tuning of an unmodified semiconductor laser," *Opt. Lett.*, vol. 13, no. 9, pp. 725–727, 1988.

[10] F. Allard, I. Maksimovic, M. Abgrall, and P. Laurent, "Automatic system to control the operation of an extended cavity diode laser," *Rev. Sci. Instrum.*, vol. 75, no. 1, pp. 54–58, Nov. 2004.

[11] Y. Ohman, "On some new auxiliary instruments in astrophysical research VI. A tentative monochromator for solar work based on the principle of selective magnetic rotation," *Stockholms Obs. Ann*, vol. 19, no. 4, pp. 9–11, 1956.

[12] P. Wanninger, E. C. Valdez, and T. M. Shay, "Diode-laser frequency stabilization based on the resonant Faraday effect," *IEEE Photon. Technol. Lett.*, vol. 4, no. 1, pp. 94–96, Jan. 1992.

[13] K. Choi, J. Menders, P. Searcy, and E. Korevaar, "Optical feedback locking of a diode laser using a cesium Faraday filter," *Opt. Commun.*, vol. 96, no. 4–6, pp. 240–244, 1993.

[14] X. Miao et al., "Note: Demonstration of an external-cavity diode laser system immune to current and temperature fluctuations," *Rev. Sci. Instrum.*, vol. 82, no. 8, 2011, Art. no. 086106.

[15] P. Chang et al., "A Faraday laser lasing on Rb 1529 nm transition," *Sci. Rep.*, vol. 7, no. 1, pp. 1–8, 2017.

[16] P. Chang et al., "A Faraday laser operating on Cs 852 nm transition," *Appl. Phys. B*, vol. 125, no. 12, pp. 1–6, 2019.

[17] M. D. Rotondaro, B. V. Zhdanov, M. K. Shaffer, and R. Knize, "Narrow-band diode laser pump module for pumping alkali vapors," *Opt. Exp.*, vol. 26, no. 8, pp. 9792–9797, 2018.

[18] H. Tang et al., "18 W ultra-narrow diode laser absolutely locked to the Rb D_2 line," *Opt. Exp.*, vol. 29, no. 23, pp. 38728–38736, 2021.

[19] K. B. MacAdam, A. Steinbach, and C. Wieman, "A narrow-band tunable diode laser system with grating feedback, and a saturated absorption spectrometer for Cs and Rb," *Am J. Phys*, vol. 60, no. 12, pp. 1098–1111, 1992.

[20] C. Wieman and T. W. Hänsch, "Doppler-free laser polarization spectroscopy," *Phys. Rev. Lett.*, vol. 36, no. 20, pp. 1170–1173, 1976.

[21] T. W. Hansch and B. Couillaud, "Laser frequency stabilization by polarization spectroscopy of a reflecting reference cavity," *Opt. Commun.*, vol. 35, no. 3, pp. 441–444, 1980.

[22] R. K. Raj, D. Bloch, J. J. Snyder, G. Camy, and M. Ducloy, "High-frequency optically heterodyned saturation spectroscopy via resonant degenerate four-wave mixing," *Phys. Rev. Lett.*, vol. 44, no. 19, pp. 1251–1254, 1980.

[23] J. Ye, L. Ma, and J. L. Hall, "Molecular iodine clock," *Phys. Rev. Lett.*, vol. 87, no. 27, 2001, Art. no. 270801.

[24] E. Zang, J. Cao, Y. Li, C. Li, and Y. Deng, "Realization of four-pass I_2 absorption cell in 532-nm optical frequency standard," *IEEE Trans. Instrum. Meas.*, vol. 56, no. 2, pp. 673–676, Apr. 2007.

[25] T. Schuldt et al., "Development of a compact optical absolute frequency reference for space with 10^{-15} instability," *Appl. Opt.*, vol. 56, no. 4, pp. 1101–1106, 2017.

[26] B. Wu et al., "Modulation transfer spectroscopy for D1 transition line of rubidium," *J. Opt. Soc. Am B*, vol. 35, no. 11, pp. 2705–2710, 2018.

[27] P. Chang, S. Zhang, H. Shang, and J. Chen, "Stabilizing diode laser to 1 Hz-level allan deviation with atomic spectroscopy for Rb four-level active optical frequency standard," *Appl. Phys. B*, vol. 125, no. 11, pp. 1–8, 2019.

[28] K. Döringshoff et al., "Iodine frequency reference on a sounding rocket," *Phys. Rev. Appl.*, vol. 11, no. 5, 2019, Art. no. 054068.

[29] T. Schuldt et al., "Optical clock technologies for global navigation satellite systems," *GPS Solutions*, vol. 25, no. 3, pp. 1–11, 2021.

[30] J. Wang, S. Yan, Y. Wang, T. Liu, and T. Zhang, "Modulation-free frequency stabilization of a grating-external-cavity diode laser by magnetically induced sub-Doppler dichroism in cesium vapor cell," *Jpn. J. Appl. Phys.*, vol. 43, no. 3, pp. 1168–1171, 2004.

[31] A. Millett-Sikking, I. G. Hughes, P. Tierney, and S. L. Cornish, "DAVLL lineshapes in atomic rubidium," *J. Phys. B: At Mol. Opt. Phys.*, vol. 40, no. 1, pp. 187–198, 2006.

[32] D. Su et al., "Application of sub-Doppler DAVLL to laser frequency stabilization in atomic cesium," *Appl. Opt.*, vol. 53, no. 30, pp. 7011–7016, 2014.

[33] R. V. Pound, "Electronic frequency stabilization of microwave oscillators," *Rev. Sci. Instrum.*, vol. 17, no. 11, pp. 490–505, 1946.

[34] R. W. P. Drever et al., "Laser phase and frequency stabilization using an optical resonator," *Appl. Phys. B*, vol. 31, no. 2, pp. 97–105, 1983.

[35] H. Shang et al., "Laser with 10^{-13} short-term instability for compact optically pumped cesium beam atomic clock," *Opt. Exp.*, vol. 28, no. 5, pp. 6868–6880, 2020.

[36] P. Chang et al., "Frequency-stabilized Faraday laser with 10^{-14} short-term instability for atomic clocks," *Appl. Phys. Lett.*, vol. 120, no. 14, 2022, Art. no. 141102.

[37] N. Ito, "Doppler-free modulation transfer spectroscopy of rubidium $5^2S_{1/2}$-$6^2P_{1/2}$ transitions using a frequency-doubled diode laser blue-light source," *Rev. Sci. Instrum.*, vol. 71, no. 7, pp. 2655–2662, 2000.

[38] H. S. Moon, L. Lee, K. Kim, and J. B. Kim, "Laser frequency stabilizations using electromagnetically induced transparency," *Appl. Phys. Lett.*, vol. 84, no. 16, pp. 3001–3003, 2004.

[39] H. S. Moon, W. K. Lee, L. Lee, and J. B. Kim, "Double resonance optical pumping spectrum and its application for frequency stabilization of a laser diode," *Appl. Phys. Lett.*, vol. 85, no. 18, pp. 3965–3967, 2004.

[40] B. Yang, J. Zhao, T. Zhang, and J. Wang, "Improvement of the spectra signal-to-noise ratio of caesium $6P_{3/2}$-$8S_{1/2}$ transition and its application in laser frequency stabilization," *J. Phys. D: Appl. Phys.*, vol. 42, no. 8, 2009, Art. no. 085111.